Meles, Mehari; Rajasekaran, Akash; Mela, Lauri; Ghazalian, Reza; Ruttik, Kalle; Jäntti, Riku

Performance evaluation of measurement based GPS denied 3D drone localization and tracking

Published in:
2023 IEEE Wireless Communications and Networking Conference (WCNC)

DOI:
10.1109/WCNC55385.2023.10118816

Published: 12/05/2023

Document Version
Peer-reviewed accepted author manuscript, also known as Final accepted manuscript or Post-print

Please cite the original version:
Meles, M., Rajasekaran, A., Mela, L., Ghazalian, R., Ruttik, K., & Jäntti, R. (2023). Performance evaluation of measurement based GPS denied 3D drone localization and tracking. In *2023 IEEE Wireless Communications and Networking Conference (WCNC)* (IEEE Wireless Communications and Networking Conference). IEEE. https://doi.org/10.1109/WCNC55385.2023.10118816

Performance evaluation of measurement based GPS denied 3D drone localization and tracking

Mehari Meles, Akash Rajasekaran, Lauri Mela, Reza Ghazalian, Kalle Ruttik, Riku Jäntti
Department of Communications and Networking, Aalto University 02150 Espoo, Finland
Email: {mehari.meles, akash.rajasekaran, lauri.mela, reza.ghazalian, kalle.ruttik, riku.jantti}@aalto.fi

***Abstract*—This paper presents experimental results of GPS free drone location using two antenna arrays. The experimental platform contains two synchronized stationary 4-by-4 rectangular antenna arrays. The arrays receive the signal emitted from a single antenna mounted on a drone. A Multiple signal classification (MUSIC) algorithm is applied to estimate the angle of arrival (AOA) at each array. The estimated AOA from both arrays is combined by the triangulation technique. We further employed the Extended Kalman Filter (EKF) to mitigate the estimated 3D location errors from the triangulation. To evaluate the performance of the AOA estimation, we conducted several measurements with different types of trajectories using a test-bed. The location estimation results of the proposed method are quantitatively compared and evaluated with the GPS trajectory of the drone. The estimation results have verified that the proposed experimental approach can localize and track the drone with reasonable accuracy.**

***Index Terms*—drone, MUSIC,AOA, Triangulation, EKF.**

I. Introduction

GPS denied drone location estimation techniques have lately become an active research field [1]. An efficient way to localize an asynchronous target is to measure time difference of arrival (TDOA) or angle of arrival (AOA) [2]. Even though TDOA based localization can be very accurate, the high performance of the algorithm can only be achieved with precise synchronization between the transmitter and receiver. AOA can operate in more relaxed environment and as such well exploited by researchers. For instance in [3] it is used for drone self-localization. Commonly Multiple signal classification (MUSIC) is applied to estimate the direction of the incoming signal.

According to [4], [5], for better 3D location estimation accuracy, MUSIC algorithm needs to have an initial values close to true elevation and azimuth angles, it is also inefficient due to high computational cost. In [6], triangulation-based 2D state location positioning, where measurements from two sensors are geometrically combined for better state estimation by deploying camera networks.

However, as stated in [7], in practice MUSIC has problems in estimating azimuth and elevation from noisy measurements, also the range cannot be estimated using one antenna array receiver as seen in [8] making it difficult to localize the drone in Cartesian coordinates. For this reason, in this paper we first apply MUSIC to measure the AOA at each array and triangulated the intersection points to estimate the location of the drone. The triangulated points are filtered by EKF. In our experimental setup, we deployed two identical antenna arrays to receive the incoming signal from the drone and used the triangulation technique from the receivers toward the unknown drone location. An EKF has been considered in [9] to realize the localization of an object by fusing odometry and laser range information.

We present a triangulation method to measure the location of the drone using the actual measured signal by the two antenna arrays. For tracking the state of the drone at each sampling, the EKF algorithm is applied. Since our antenna arrays are sensitive to height estimation, especially in up/down trajectory, we fused the barometer reading and height from the triangulation in the update step of the EKF. From the experimental measurement, the results of the MUSIC for each array, triangulation of the two arrays, and EKF tracking are evaluated separately.

The structure of this paper is provided as: In Section II, the whole localization algorithms supported with block diagram is provided. In Section III, the outdoor measurement setup of the drone flight and the position of antenna arrays is discussed. The signal model transmitted from the drone and AOA estimation using MUSIC and triangulation for both azimuth and elevation at the receiver is given in Section IV. The location estimation results and conclusions are given in Section V and Section VI, respectively.

II. Localization algorithms

Here, we provided the employed algorithms and models of the 3D drone localization. We considered a drone equipped with an monopole antenna and two stationary 4- by- 4 element arrays constructed from identical dipole antennas. Both stationary antenna arrays are positioned at known locations and signals from them are synchronized. They both see the drone, ie. the signal from drone is on line of sight (LOS). All the antenna elements from both antenna arrays are connected to a vector network analyzer (VNA). Antenna at the drone operates as transmitter of the VNA. The VNA cables limit the distance between the two arrays and the drone, as shown in Fig. 2. The complex received signals from all the elements from both arrays are timestamped and stored for the post processing.

The drone localization process considered here is based on two URA arrays located in different coordinate systems. The arrays measure AOA of the drone signal. The URA receivers are 13 meters apart in x-direction and have LOS with the drone. The signals received by each antenna element in the arrays are processed by MUSIC algorithm for AOA estimation. The AOA measurements are then utilized to estimate the position of the drone based on the triangulation technique. Triangulation is applied to find the intersection of the two lines from each array towards the drone, which depends on the measured azimuth and elevation angles. Due to the fact that the measurement during the drone trajectory is nonlinear, we applied EKF algorithm to track the state of the drone while it transmits signal in every sampling. Fig. 1 shows the block diagram of the drone localization and tracking applied in this paper.

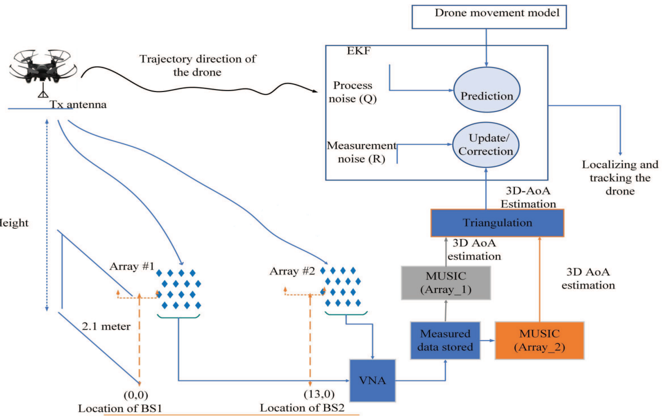

Fig. 1: Block diagram of the localization process.

III. Measurement setup and drone trajectories

In this measurement setup, we followed certain procedures. As shown in Fig.3, we positioned the first and second antenna arrays at the coordinates $(0,0,2.1)$ and $(13,0,2.1)$, respectively. We also measured the distance from the location of the first array towards the starting point of the planned trajectory of the drone, as shown in Fig. 2. Before the experiment was performed, we first calibrated the measurement equipment. For validation purposes, we transmit and receive signals while the drone was kept stationary on the ground, i.e before flying.

We performed several measurements by flying the drone with different patterns of trajectories within specific periods. The whole measurement setup employs 4 port R&S ZNB8 VNA and R&S ZN-Z84 switch matrix, which connect the cables to antennas used in a test-bed. The ZN-Z84 are used to expand the number of ports in the tets-bed to 48, and the antenna equipped on the flying drone is connected by a long coaxial cable. For each 4×4 antenna array, 16 identical coaxial cables are connected, and before the measurements are performed, system calibration of the testbed, R&S ZV-Z51, was made. The advantage of this calibration avoids the effect of the cables and by doing this the measurement results will be influenced only by the measurement system noise and radio channels.

Having completed the setup, we flew the drone and controlled the measurement remotely with a laptop. During the measurement of one sample, the received signal from each array element is collected synchronously. Also, While the VNA measurements are executed, all the drone navigation information is recorded and saved on the PC for comparison and validation. To accomplish measurements with elements of the arrays, the ports of antenna arrays is increased using Switch matrix units, However, they are not consistently used to perform simultaneous measurements for every element of the arrays and due to this at most three elements are measured at a time. but, using single frequency with very fast switching of the RF switches which enables to measure from every antenna element of the array. During the flight of the drone, the GPS data, the received signal by both antenna arrays, sampling time, and frequency transmission were collected.

Fig. 2: Outdoor experimental setup.

IV. Proposed Methodology

A. AOA Estimation Algorithm

In this subsection, we evaluate the 3D AOA estimation and localization accuracy of our experiment.

1) Antenna Array Model:
AOA of an incoming signal can be estimated using different structures of antenna arrays, for instance uniform rectangular arrays (URA), uniform circular arrays (UCA) and uniform linear arrays (ULA).

In this paper, two synchronized URAs with identical antenna elements. The two rectangular arrays are positioned in the xz-plane, as shown in Fig. 3, which has M_x and M_z antenna elements in the directions of x and z , respectively. All the antenna elements of the arrays have spacing d_x and d_z in x and z, respectively. Both array receivers are deigned with spacing of $\lambda/2$ in both x and z axes, and a $\lambda/4$ offset towards the x axis. The estimated azimuth and elevation angles of the two arrays are denoted by ϕ_i and θ_i respectively, where $i=1,2$ represent for first and second arrays, respectively.

Generally, the received signal by both arrays at k snapshot can be modeled as a function of the ϕ and θ as:

$$y_{i,k} = A_{i,k}(\theta_{i,k},\phi_{i,k})S + n_{i,k}, i=1,2 \tag{1}$$

where:

- $y_{i,k}$: received signal.
- $A_{i.k}$: steering vector.
- S : transmitted signal from the drone.
- $n_{i,k}$: noise vector.
- $\theta_{i,k}$: elevation angle.
- ϕ_i, k : azimuth angle.

The array vector of the model given in (1) can be expressed:

$$A(\theta_i,\phi_i) = [a(\theta_{i,1},\phi_{i,1}); a(\theta_{i,2},\phi_{i,2}); \ldots, a(\theta_{i,k},\phi_{i,k})] \tag{2}$$

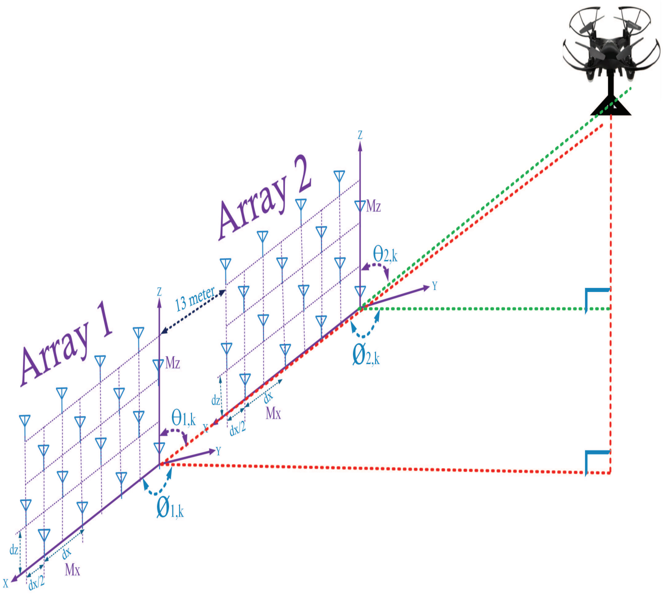

Fig. 3: Position of the two arrays.

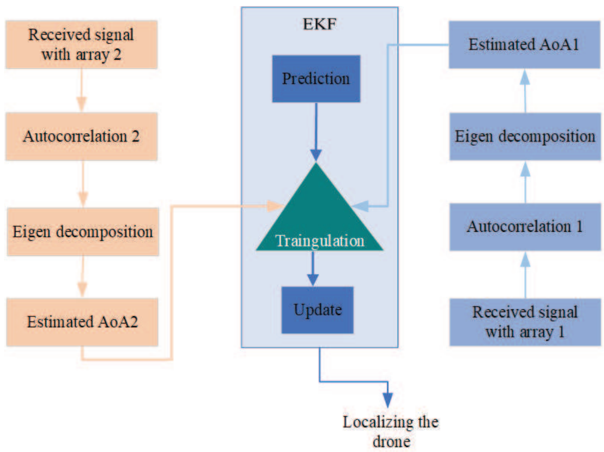

Fig. 4: MUSIC and triangulation integration

2) MUSIC algorithm:

We applied MUSIC [10] to measure the 3D location of the drone in our experiment. As can be seen in Fig. 4, the complex signal received by the two arrays is fed to MUSIC, which performs autocorrelation and eigendecomposition sequentially, resulting in a direction estimation. Once the AOA is estimated from both arrays, the state is updated with the measured/triangulation in every snapshot. The autocorrelation (1) is:

$$R_{yy,i,k} = \frac{1}{N}\sum_{k=1}^{N} y_{i,k}(kT_s)y_{i,k}^{H}(kT_s), i = 1,2. \tag{3}$$

N, H, and T_s are the number of sampling, Hermitian conjugate transpose and snapshot respectively. Here, eigenvalue decomposition is applied to the autocorrelation matrix (3), and then sorting the eigenvectors in a descending order in terms of the magnitude of corresponding eigenvalues of the measured signal from each array. The MUSIC is applied to measure the direction of the signal in the azimuth & elevation planes for both arrays. After decomposing the corresponding associated source matrix and noise matrix of (3), the first M eigenvector and the last eigenvector is called the signal space and noise space respectively. From the orthogonality of the the steering vector and noise subspace [11], the AOA is evaluated by the peak values of the MUSIC spatial spectrum.

$$P(\theta_{i,k},\phi_{i,k}) = \frac{V^*(\theta_{i,k},\phi_{i,k})V(\theta_{i,k},\phi_{i,k})}{V^*(\theta_{i,k},\phi_{i,k})E_{n,i,k}E^*_{n,i,k}V(\theta_{i,k},\phi_{i,k})}, i = 1,2.$$

$V^*(\theta_{i,k},\phi_{i,k})$ and E_n defines the array response vectors and noise-subspace respectively. In (4), the peak points of the spectrum minimize the $E_n^*V(\theta_{i,k},\phi_{i,k})$ in the 3D space, in which the location of the drone is estimated.

3) Triangulation:

After we collect the measured signal from the two arrays, we employed the triangulation technique to measure the direction of the transmitter, i.e. drone. Let the location of the stationary identical arrays be denoted as Ar_i with coordinates of $(x_i, y_i, z_i, i = 1,2)$. Recall the expression given in (1), $\theta_{i,k}$, and $\phi_{i,k}$ define the associated elevation and azimuth angles, respectively. Let D_k with (x_k, y_k, z_k) coordinates be the transmitting location of the hovering drone, where k is the number of snapshots. The measured azimuth and elevation angles from the arrays (Ar_i) to the drone (D_k) are $\phi_{i,k}$ and $\theta_{i,k}$ respectively. The localization of the drone is performed based on the AOAs at both arrays from the self- transmitting drone.

As shown in Fig.3, the drone position can be estimated on the line through the two arrays Ar_i in the direction of $(\theta_{i,k},\phi_{i,k})$ in the spherical coordinate system. Formulating the two lines using 3D functions $F_{i,k}(x,y,z)$, the intersection of $F_{1,k}$ and $F_{2,k}$ is the estimated location of the drone. We can express the direction of the incoming signal in cartesian coordinate systems:

$$\begin{bmatrix} x_{i,k} \\ y_{i,k} \\ z_{i,k} \end{bmatrix} = \begin{bmatrix} \cos(\theta_{i,k})\cos(\phi_{i,k}) \\ \cos(\theta_{i,k})\sin(\phi_{i,k}) \\ \sin(\theta_{i,k}) \end{bmatrix} \tag{4}$$

Let's assume that the line L_1 passes through the point of the coordinate of the first array (Ar_1), (x_1, y_1, z_1) in the direction a_1, a_2, a_3 towards the unknown coordinate of the drone (x_k, y_k, z_k). Now, we can express the 3D Parametric form:

$$\frac{x_k - x_1}{a_1} = \frac{y_k - y_1}{a_2} = \frac{z_k - z_1}{a_3} = t \tag{5}$$

t is a parameter describing a particular point on the line L_1.

Similarly, for the second array (A_{r2}), using a symmetric form we have the relation:

$$\frac{x_k - x_2}{b_1} = \frac{y_k - y_2}{b_2} = \frac{z_k - z_2}{b_3} \tag{6}$$

b_1, b_2, and b_3 denote the direction vector from the second array towards the drone. Substituting (6) in (5) and solving for t, the measured location of the drone is evaluated in cartesian coordinate system and this is fed to the extended Kalman filter as an observation model.

B. Extended Kalman Filter (EKF)

EKF is an extended algorithm of the KF, which linearizes the nonlinear model at the current mean and covariance using first order Taylor series. As stated in [12], [13], the linearized version of the nonlinear state model is applied for the state estimation using EKF. The process model governed by the linear stochastic is formulated:

$$x_k = A_{k-1}x_{k-1} + B_{k-1}u_{k-1} + w_{k-1}, \tag{7}$$

$w_{k-1} \sim \mathcal{N}(0, Q_k)$ is the process noise, which is a normal distribution with zero mean and covariance matrix Q_k, and x_k and x_{k-1} are the current and previous state at snapshot k and $k-1$, respectively. Vector A represents a state transition matrix, and B is control input matrix applied to a dynamic control vector u_{k-1}, and the corresponding matrix expression is provided in [14].

The measurement model of the EKF is:

$$z_k = h(x_k) + v_k, \tag{8}$$

$v_k \sim \mathcal{N}(0, R_k)$ is the measurement noise, also a normal distribution with zero mean and covariance matrix R_k, and z_k is also the observation model, which depends on the state model. The functions $h(x_k)$ is the nonlinear measurement transition matrix and the corresponding jacobian matrices of the measurement model:

$$H_k = \frac{\partial h}{\partial x} | \; x_k, \tag{9}$$

Applying the partial derivatives of (9), the elements of measurement transition matrix can be represented as:

$$H_k = \begin{bmatrix} \frac{x_k}{\sqrt{x_k^2+y_k^2+z_k^2}} & \frac{y_k}{\sqrt{x_k^2+y_k^2+z_k^2}} & \frac{z_k}{\sqrt{x_k^2+y_k^2+z_k^2}} & \\ \frac{y_k}{x_k^2+y_k^2} & \frac{-x_k}{x_k^2+y_k^2} & 0 & 0_{3\times3} \\ \frac{-x_k z_k}{(x_k^2+y_k^2+z_k^2)\sqrt{x_k^2+y_k^2}} & \frac{-y_k z_k}{(x_k^2+y_k^2+z_k^2)\sqrt{x_k^2+y_k^2}} & \frac{\sqrt{x_k^2+y_k^2}}{x_k^2+y_k^2} & \end{bmatrix} \tag{10}$$

H_k is a linear measurement matrix.

The observation state can be also formulated in spherical coordinates:

$$h(x_k) = [\theta_k, \phi_k, r_k]^T, \tag{11}$$

r_k is LOS distance from the drone to array.
Then, the transition matrix in spherical coordinate is:

$$h(x_k) = \begin{bmatrix} \tan^{-1}(\frac{y_k}{x_k}) \\ \tan^{-1}(\frac{z_k}{\sqrt{(x_k)^2+(y_k)^2}}) \\ \sqrt{x_k^2+y_k^2+z_k^2} \end{bmatrix} + \begin{bmatrix} v_\theta \\ v_\phi \\ v_r \end{bmatrix}, \tag{12}$$

v_θ,v_ϕ, and v_r are mutually uncorrelated noises with zero-mean and variances of σ_θ^2, σ_ϕ^2 and σ_r^2, respectively.

Once linearization of the non-linear measurement function and the dynamic model is performed, the process of the EKF can be evaluated step by step.

1) Prediction step:

This is the first phase of the EKF, where we first predict the state $\hat{x}_k^-$ from the previous state information $\hat{x}_{k-1}$:

$$\hat{x}_k^- = A_{k-1}\hat{x}_{k-1} + B_{k-1}u_{k-1}, \tag{13}$$

$\hat{x}_k^-$ is the predicted value before the measurement is made. After this step, we find the state prediction covariance matrix based on the previous covariance (P_{k-1}) matrix [15].

$$P_k^- = A_{k-1}P_{k-1}A_{k-1}^T + Q_{k-1}, \tag{14}$$

P_k^- is the current state covariance matrix.

2) Correction step:

In this phase, the state and covariance matrix of the state are corrected by introducing new measurements. The level of the variance is evaluated by Kalman gain, κ_k:

$$\kappa_k = P_k^- H_k^T (H_k P_k^- H_k^T + R_k)^{-1}, \tag{15}$$

H_k is defined in (10).

3) Updated step:

The final state ($\hat{x}_k$) is estimated by updating the predicted state ($\hat{x}_k^-$) given in (13) using the Kalman gain and new measurement:

$$\hat{x}_k = \hat{x}_k^- + \kappa_k(z_k - h(\hat{x}_k^-)), \tag{16}$$

$h(\hat{x}_k^-)$ denote the expected measurement and z_k is defined in (8). Using the Kalman gain κ_k, we update the state covariance matrix (P_k^-):

$$P_k = (I - \kappa_k H_k)P_k^-, \tag{17}$$

P_k is the covariance of the state after new measurement is applied. Substituting (16) and (17) back in the (13) and (14) respectively, to iterate for all snapshots in the measurements.

V. Measurement Results

We validated our proposed approach first using simulation of different types of drone trajectories, after which we performed experimental/measurement based drone localization. To observe the efficiency of the proposed method, we performed several measurements with different drone trajectories, namely linear, zigzag, and up/down trajectories as provided in Fig.5, Fig.6 and Fig.7, respectively. All measurements were taken with 0.5 seconds of sampling. Fig. 5 shows a linear drone trajectory with a back-and-forth pattern, and it can be seen that the measured/triangulation from the two arrays track the drone with fluctuating bias. The noise in back-and-forth trajectory, however, is suppressed by the EKF, as shown in Fig. 5(a).

To validate the efficiency of our methodology, we measured by maintaining a zigzag drone trajectory path, following X direction with significant changes also in the Y direction, as shown in Fig 6(b).

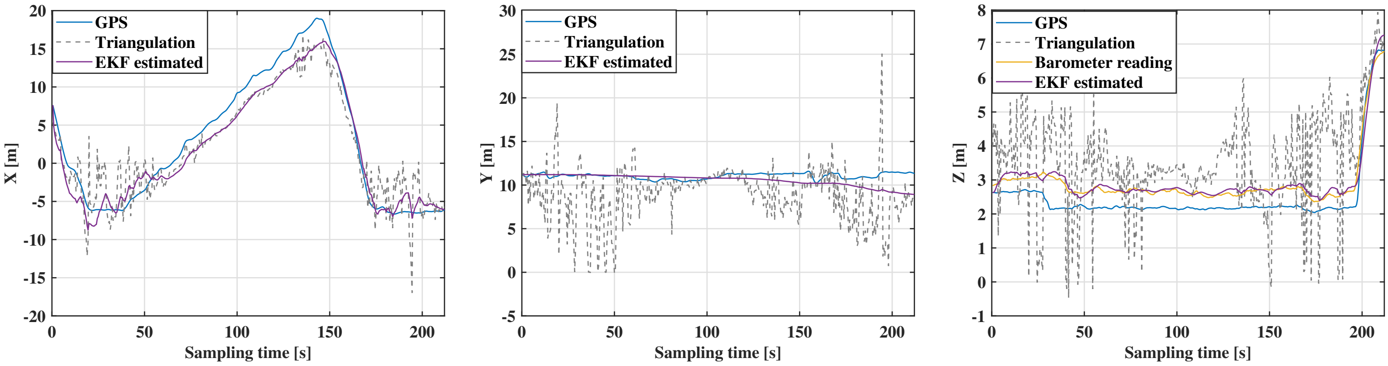

(a) (b) (c)

Fig. 5: Results of linear trajectory; a). X-coordinate, b). Y-coordinate, c). Z-coordinate

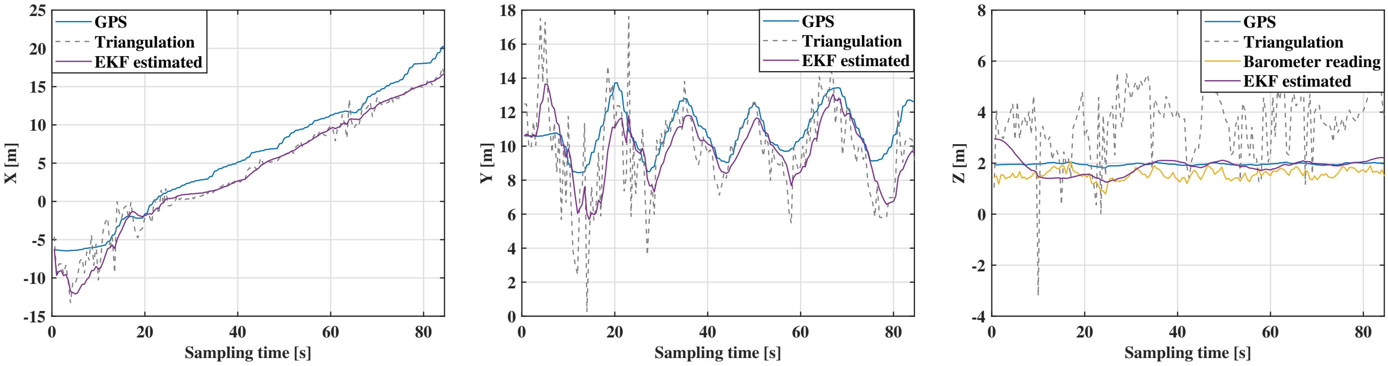

(a) (b) (c)

Fig. 6: Results of zigzag trajectory; a). X-coordinate, b). Y-coordinate, c). Z-coordinate

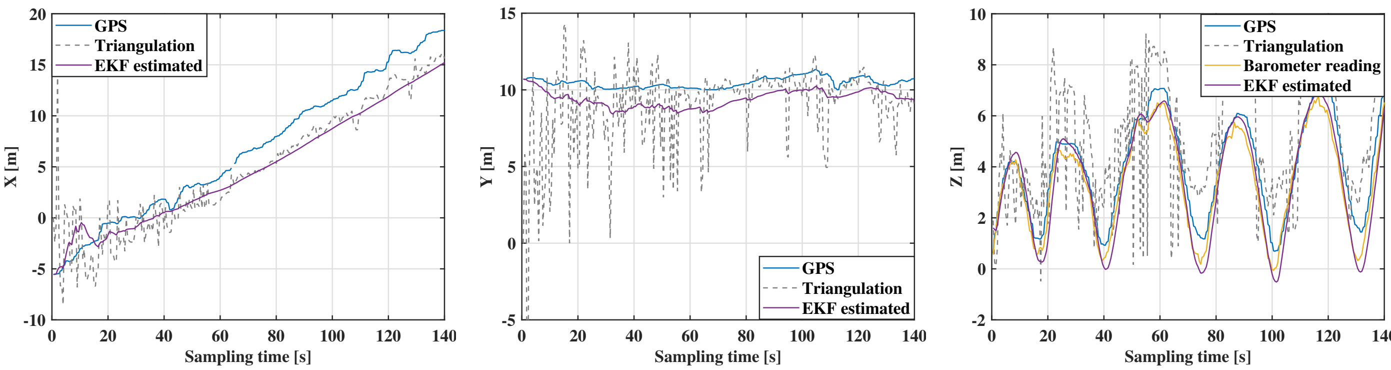

(a) (b) (c)

Fig. 7: Results of up and down trajectory; a). X-coordinate, b). Y-coordinate, c). Z-coordinate

Fig.7 shows the up/down trajectory measurements, where the height of the drone changes every snapshot. Since the array receivers are sensitive to height measurement, the measured/triangulation values are noisy. For this reason, we have two correction and update steps. In the first step the measurements from the triangulation are used, and then the height determined from the barometer is used to update the height for all trajectories, as shown in Fig. 5(c), Fig. 6(c) and Fig. 7(c). For all height estimation plots, it can be observed that the bias is significantly improved by fusing the measured height from the two arrays and barometer readings. n, we use the barometer to determine the relative height which is then fed in to the EKF as a second update step for all trajectories.

Fig.8 shows the comparison of the location error distribution

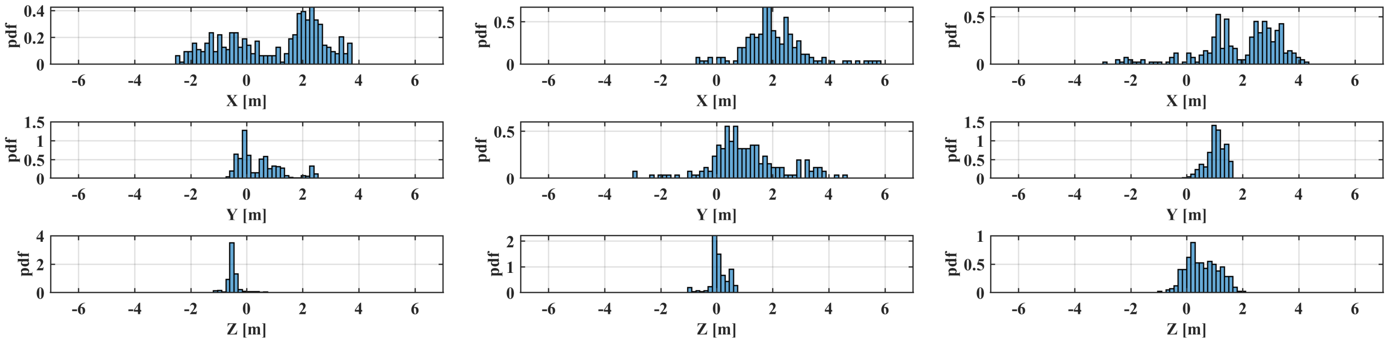

(a) (b) (c)

Fig. 8: Error distribution; a). Linear trajectory, b). Zigzag trajectory, c) Up/Down trajectory.

of the 3D coordinates for all measurements, after filtering by EKF. Although the measurement of the height is noisy for all types of trajectories, its location mean error is far less than the X & Y, and this accuracy improvement happens due to the fusing.

VI. Conclusion

In this work, we evaluated the performance of measurement-based GPS denied drone localization and tracking. Our system consists of two synchronized antenna arrays for receiving signals and a single antenna transmitter mounted on the drone itself. Once the signal is received, we employed MUSIC algorithm at each antenna array to estimate the direction of the transmitter/drone. Triangulation is performed based on the angles measured by the two arrays to estimate the 3D location of the drone. To improve the accuracy of position estimations of the drone, the results of the triangulation from the two arrays is used as a measurement model for the EKF algorithm. We evaluated our approach using different types of drone trajectories with two antenna array receivers. We demonstrate that our approach is effective for practical drone localization and tracking. We plan to extend this paper by deploying multiple arrays with a greater distance between them and the drone.

References

[1] Sinan Gezici, *"A survey on wireless position estimation."* Wireless personal communications 44.3 (2008): 263-282.

[2] Siamak Yousefi, Xiao-Wen Chang, and Benoit Champagne. *"An improved extended Kalman filter for localization of a mobile node with NLOS anchors."* Proceedings of the Ninth International Conference on Wireless and Mobile Communications (ICWMC). 2013.

[3] Mehari Meles, Akash Rajasekaran, Kalle Ruttik, Reino Virrankoski, and Riku Jäntti. *"Measurement based performance evaluation of drone self-localization using AoA of cellular signals."* In 2021 24th International Symposium on Wireless Personal Multimedia Communications (WPMC), pp. 1-5. IEEE, 2021.

[4] Shohei Kikuchi, Hiroyuki Tsuji, and Akira Sano. *"Pair-matching method for estimating 2-D angle of arrival with a cross-correlation matrix."*, IEEE Antennas and Wireless Propagation Letters 5 (2006): 35-40.

[5] QI Cheng and Yingbo Hua. *"Further study of the pencil-MUSIC algorithm."* IEEE Transactions on Aerospace and Electronic Systems 32.1 (1996): 284-299.

[6] Onur Tekdas and Volkan Isler. *"Sensor placement for triangulation-based localization."* IEEE transactions on Automation Science and Engineering 7.3 (2010): 681-685.

[7] Jin Chen, Sheng Guan, Ying Tong, and Lei Yan. *"Two-dimensional direction of arrival estimation for improved archimedean spiral array with MUSIC algorithm."* IEEE Access 6 (2018): 49740-49745.

[8] Mehari Meles, Lauri Mela, Akash Rajasekaran, Kalle Ruttik, and Riku Jäntti. *"Drone localization based on 3D-AoA signal measurements."* In 2022 IEEE 95th Vehicular Technology Conference:(VTC2022-Spring), pp. 1-5.IEEE, 2022.

[9] Ling Chen, Huosheng Hu, and Klaus McDonald-Maier. *"Ekf based mobile robot localization."* 2012 Third International Conference on Emerging Security Technologies. IEEE, 2012.

[10] I. Stevanovíc, A. Skrivervik, and J. R. Mosig. *"Introduction to Smart Antennas."* Morgan & Claypool, San Rafael (2007).

[11] P Laxmikanth,S Susruthababu, L Surendra, S Suparshya Babu, and D Venkata Ratnam. *"Enhancing the performance of AOA estimation in wireless communication using the MUSIC algorithm."* 2015 International Conference on Signal Processing and Communication Engineering Systems. IEEE, 2015.

[12] Jitendra R Raol, Girija Gopalratnam, and Bhekisipho Twala.*" Nonlinear filtering: concepts and engineering applications"*. CRC Press, 2017.

[13] Milca F Coelho, Kouamana Bousson, and Kawser Ahmed. *"Survey of nonlinear state estimation in aerospace systems with Gaussian priors."* Advances in aircraft and spacecraft science 7.6 (2020): 495-516.

[14] Youngjoo Kim and Hyochoong Bang. *"Introduction to Kalman filter and its applications."* Introduction and Implementations of the Kalman Filter 1 (2018): 1-16.

[15] Yaakov Bar-Shalom, X. Rong Li, and Thiagalingam Kirubarajan. *"Estimation with applications to tracking and navigation: theory algorithms and software"*. John Wiley & Sons, 2004.